ISSN 0020-4412, Instruments and Experimental Techniques, 2018, Vol. 61, No. 1, pp. 68–74. © Pleiades Publishing, Ltd., 2018.
Original Russian Text © Yu.A. Andreev, A.M. Efremov, M.Yu. Zorkaltseva, V.I. Koshelev, A.A. Petkun, 2018, published in Pribory i Tekhnika Eksperimenta, 2018, No. 1, pp. 60–67.

ELECTRONICS AND RADIO ENGINEERING

Radiation of High-power Ultrawideband Pulses with Elliptical Polarization by a Conical Helical Antenna

Yu. A. Andreev, A. M. Efremov, M. Yu. Zorkaltseva, V. I. Koshelev*, and A. A. Petkun
Institute of High Current Electronics, Siberian Branch, Russian Academy of Sciences, Tomsk, 634055 Russia
**e-mail: koshelev@lhfe.hcei.tsc.ru*
Received April 3, 2017

Abstract—A high-power source of ultrawideband radiation with elliptical polarization was developed on the basis of exciting a conical helical antenna by a bipolar voltage pulse with a length of 1 ns. The antenna parameters were preliminarily estimated using analytical formulas and then optimized via numerical simulation. The results of low-voltage test measurements were compared with the data that were obtained using a program that was developed on the basis of the finite-difference method in the time domain. In high-voltage measurements, the energy efficiency of the radiator was 0.85 and the coefficient of the hodograph ellipticity measured along the antenna axis was 0.9. The effective radiation potential of the source at an amplitude of bipolar voltage pulses of 190 kV was 270 kV, while the efficiency with respect to the peak field strength was 1.35. The high-power source of ultrawideband radiation operated at a pulse repetition frequency of 100 Hz.

DOI: 10.1134/S0020441218010116

INTRODUCTION

Ultrawideband (UWB) pulses are widely used in radar to obtain a good spatial resolution and increase the amount of information about sensed objects and media. The trend of using subnanosecond UWB pulses is observed. Another important field of application of UWB pulses is the study of the susceptibility of electronic equipment to the action of electromagnetic fields. Here, nanosecond pulses are mainly used to obtain the response of electronic equipment.

To increase the radar range in radiolocation and study the stability of electronic equipment under the effects of high-intensity fields, high-power (HP) sources of UWB radiation should be developed. The main parameter for the evaluation of a HP source is the effective radiation potential, which is defined as the product rE_p, where E_p is the peak electric-field strength at the distance r in the far-field zone.

Highly efficient powerful sources with linear polarization have been created on the basis of single combined antennas for radiating nanosecond [1] and subnanosecond [2] pulses, as well as on the basis of combined antenna arrays that are excited by bipolar voltage pulses with durations of 0.2–3 ns [3]. As a result of these studies UWB pulses with the effective radiation potential $rE_p = 4.3$ MV [4] were obtained.

Investigations on the creation of HP UWB radiation sources with elliptical polarization are underway [5–7]. The elliptical polarization of radiation provides a number of advantages compared to linear polarization. First, the use of transmitting and receiving antennas with the left-hand (the electric-field vector rotates counterclockwise) and right-hand polarization provides the polarization isolation of transmitted and received signals. Second, the continuous rotation of the electric-field vector in the space makes it possible to influence objects at all angles without mechanically turning the transmitting antenna, thus allowing a reduction of the time spent on research and improving the efficiency of the test systems.

An HP UWB radiation source with elliptical polarization was created at the Institute of High Current Electronics on the basis of a single cylindrical helical antenna, which is excited by a 1-ns-long bipolar pulse [8]. When the amplitude of the generator voltage pulse was ~200 kV and the pulse repetition frequency was 100 Hz, an effective radiation potential of 280 kV was obtained. The performed research made it possible to create an HP source on the basis of a square lattice (2 × 2) of cylindrical helical antennas. When the amplitude of an exciting bipolar pulse was 225 kV, an effective radiation potential of 440 kV was obtained for a repetition frequency of 100 Hz [9].

To extend the bandwidth of the radiation frequencies, it is possible to use a conical helical antenna with a linear variation of the radius. The frequency band of a conical antenna is approximately determined by the ratio of the larger and lesser average diameters of turns d_{max}/d_{min}; however, the choice of the mode of excitation has a great effect on the radiation characteristics.

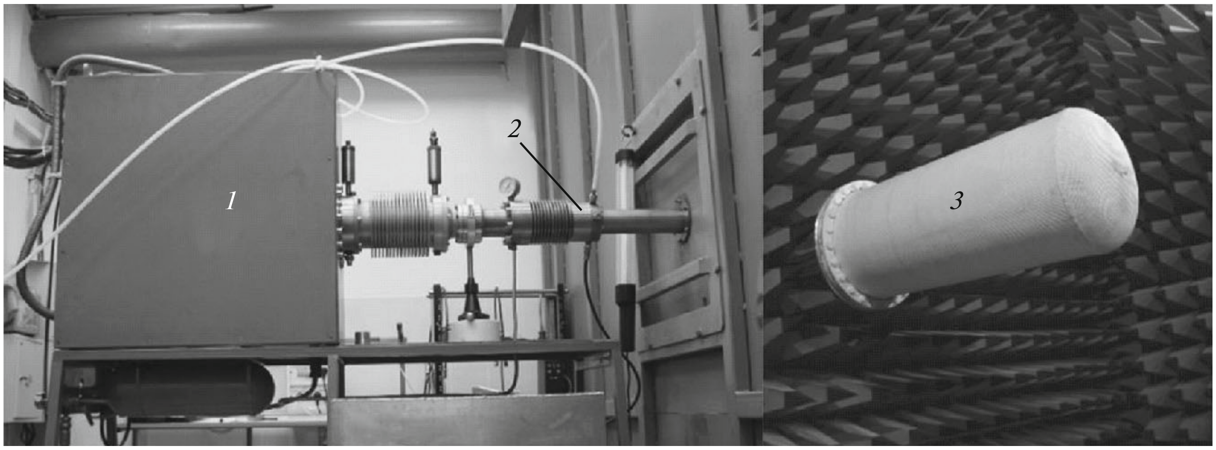

Fig. 1. The UWB radiation source with a conical helical antenna: (*1*) unipolar-pulse generator; (*2*) bipolar-pulse shaper; and (*3*) conical antenna in a dielectric container.

The authors of [10] presented theoretical and experimental studies of linear conical antennas in the frequency domain under different methods of their excitation. Studies have shown that the widest operating band corresponds to an antenna excited from the top on the side of the small diameter d_{min} of a turn through a feeder, which passes along the antenna axis. However, the characteristics of the directivity of an antenna that is excited from the base on the side of the larger diameter d_{max} of the turn were better, since in this case, the influence of the feeder is eliminated.

The objective of this study was to develop and investigate an HP UWB radiation source with elliptical polarization based on the excitation of a conical helical antenna by a high-voltage bipolar pulse of nanosecond duration. Considerable attention is drawn to numerical and experimental studies of the radiator.

1. DESIGN OF A HIGH-POWER UWB RADIATION SOURCE

The HP UWB radiation source with elliptical polarization (Fig. 1) consists of a Sinus-160 generator of high-voltage unipolar pulses (*1*), a bipolar-pulse shaper (*2*), and a transmitting conical helical antenna in a dielectric container (*3*). To increase the electric strength of the dielectric container, it was manufactured inside of glass fiber and filled the SF_6 gas to a pressure of 3 atm. The source operated at a pulse repetition rate of 100 Hz. The design of the unipolar-pulse generator and the bipolar-pulse (1 ns) shaper were considered in detail in [8].

The geometry of the transmitting antenna of the HP source is shown in Fig. 2a. The radius ρ that determines the distance from the vertex of the cone to the points of the conductor is estimated from the formula:

$$\rho(\varphi) = \rho_0 + b\varphi,$$

where ρ_0 is the radial distance from the cone vertex to the smaller cone base and b is the parameter that determines the ρ_0 change rate.

The antenna parameters were chosen for the optimal emission of a bipolar pulse with a duration of 1 ns. When the antenna parameters were selected, the recommendations given in [10, 11] and the results of the numerical simulation according to the finite-difference method in the time domain were used.The maximum and minimum outer diameters were $d_{max} = 12$ cm and $d_{min} = 5.8$ cm, respectively. The half-angle of the cone was $\theta_0 \approx 2.5°$. The interturn distance was estimated from the formula $S = 1/3\lambda_0\cos\theta_0$ (λ_0 is the wavelength that corresponds to the center frequency of the bipolar-pulse spectrum) and was found to be 10 cm. The diameter of the antenna shield and conductor were, respectively, $D = 36$ cm and $a = 1$ cm. The number of turns was $N = 7$. The appearance of the antenna is shown in Fig. 2b. The method of exciting a conical antenna from the side of the larger base is most suitable for use in HP sources. In this case, the mechanical stability of the antenna increases and it becomes unnecessary to use a feeder that extends along the axis, which is an electric monopole and impairs the directivity characteristics of the antenna.

2. THE CONICAL HELICAL ANTENNA

The characteristics of antenna matching to a coaxial feeder with a characteristic impedance of 50 Ω were estimated in a numerical calculation. Numerical studies of antennas with different diameters d_{max} and d_{min} showed that upon excitation from the side of the larger diameter, the small diameter has a weak effect on the characteristics of matching to the feeder. In this case, the lower cutoff frequency of the frequency dependence of the voltage standing-wave ratio (VSWR) is determined by the larger diameter.

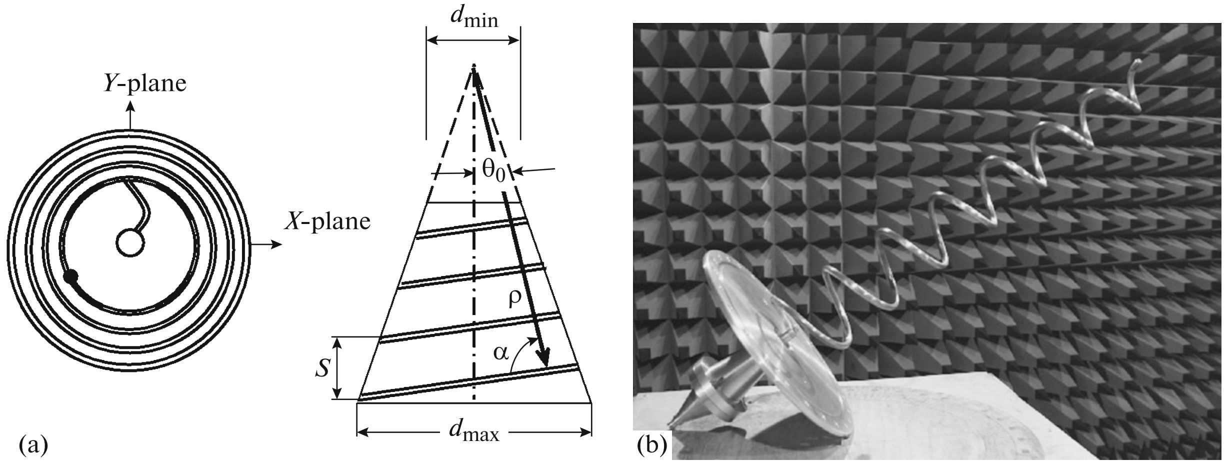

Fig. 2. (a) The geometry and (b) appearance of the conical helical antenna: (d_{max}, d_{min}) the maximum and minimum outer diameters of the conical antenna, (θ_0) half-angle of the cone, and (α) conductor winding angle.

Experimental measurements of the matching characteristics were conducted using an Agilent N5227A meter of complex transmission coefficients. The use of an impedance transformer between the coaxial input of the antenna and its first turn in the antenna design allowed the matching bandwidth to be extended. For the ratio of the diameters $d_{max}/d_{min} = 2.1$ that determines the radiation bandwidth, the frequency overlap coefficient for a VSWR level of at most 2 in the experiment was $b_f = 3.85$. The calculated and experimental frequency dependences of the VSWR are shown in Fig. 3. The difference between the calculated and experimental curves, especially at high frequencies, can be explained by the incomplete conformity of the geometry of the radiators.

Numerical and experimental investigations of the radiation characteristics of a conical antenna were performed. Figure 2a shows the planes in which the radiation characteristics were investigated. Here, a dot marks the end of the conductor of the helical antenna. The experimental studies were carried out in an anechoic chamber using a low-voltage generator of bipolar pulses with a duration of 1 ns. The radiated pulses were registered using a LeCroy Wave Master 830Zi-A oscilloscope with a bandwidth of up to 30 GHz. Two symmetric dipoles that were crossed at a right angle [12] and a TEM antenna were used in the measurements.

A small deflection of the turns of the conical helix ($\theta_0 \approx 2.5°$) from the cylindrical generatrix allows one to presume the presence of a conditional radiation center. The technique for determining the radiation center for a cylindrical helical antenna was described in [8]. For the radiation direction $\theta = 0°$ and the assumption that the radiation center lies on the antenna axis, the dependences of the effective radiation potential $(r - r_0)E_p$ on the distance r were obtained in computations and experiments, which differed in the reference point r_0. The point r_0 that is measured from the antenna shield and for which the criterion $(r - r_0)E_p \approx$ const is reached at a minimum distance r will be considered as the radiation center.

Figure 4a shows the calculated curves of the dependence $(r - r_0)E_p(r)$ that were obtained under excitation by a bipolar pulse of nanosecond duration. Curve *1* corresponds to the case where the reference point was $r_0 = 0$, curve *2* was obtained at $r_0 = 10$ cm, curve *3* corresponds to $r_0 = 24$ cm, and curve *4* was obtained at $r_0 = 73$ cm (the helix end). Calculations showed that the point $r_0 = 24$ cm corresponds to the antenna radiation center. Analogous dependences that were obtained experimentally are shown in Fig. 4b. As a result of the experiments, the point with the distance $r_0 = 20$ cm was assumed to be the radiation center, which is close to the calculation result. In Figs. 4a and

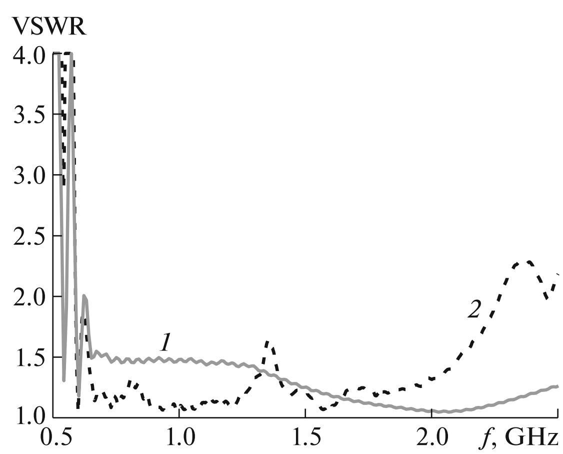

Fig. 3. The frequency dependences of the VSWR for the conical helical antenna: (*1*) calculation and (*2*) experiment.

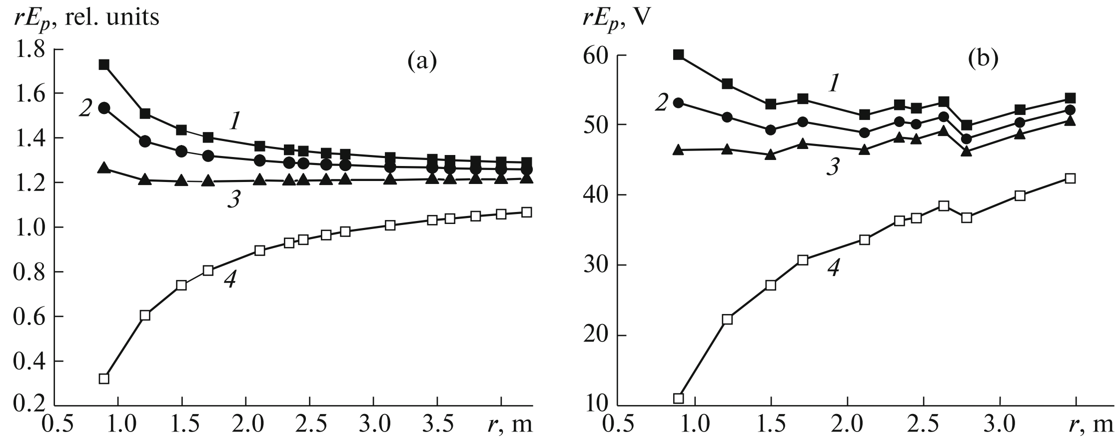

Fig. 4. (a) The calculated and (b) experimental dependences of $(r - r_0)E_p$ on the distance along the axis of the conical helical antenna: (*1*) reference point relative to the ground plate $r_0 = 0$, (*2*) 10, (*3*) 24 (calculation) and 20 (experiment), and (*4*) 73 cm.

4b, all distances were corrected so that the ground plates served as the reference point for all curves.

The additional criterion $p(r) \approx$ const [8], where p is the coefficient of ellipticity equal to the ratio of the minor axis of the hodograph to the major axis, was used to find the position of the boundary of the far-field zone of the conical antenna. The minor and major axes were chosen for the outer polarization ellipse of the hodograph that was measured in the time domain.

Figure 5 shows the calculated (curve *1*) and experimental (curve *2*) dependences $p(r)$ that were obtained for the radiation direction $\theta = 0°$. The calculation showed that the position of the boundary of the far-field zone that satisfies the criterion $p(r) \approx$ const corresponds to the distance from the antenna shield $r_d \approx$ 1.5 m. The experimental curve was constructed according to the measurement results (marked with dots in Fig. 5) using the regression method. It follows from the experimental data that the position of the boundary of the far-field zone corresponds to the distance from the ground plate $r_d \approx 2$ m, which is close to the calculated value. Figure 6 shows the calculated and experimental hodographs that were obtained at the distance $r = 2.8$ m from the ground plate in the direction $\theta = 0°$; the coefficients of ellipticity of the calculated and experimental hodographs were $p \cong 0.91$ and $p \cong 0.95$, respectively.

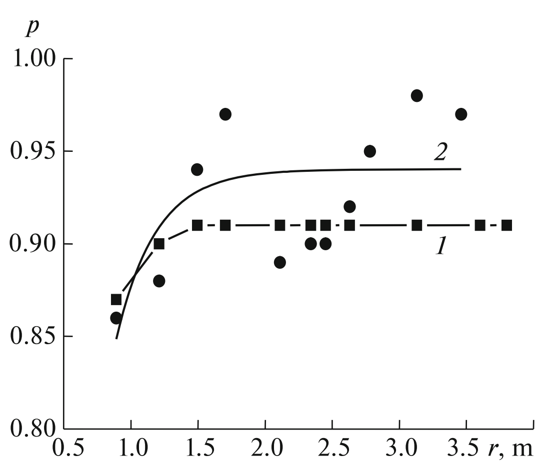

Fig. 5. The (*1*) calculated and (*2*) experimental dependences of the coefficient of ellipticity on the distance in the direction $\theta = 0°$.

When a high-power UWB source was used in practice, it seemed to be necessary to know the position of the boundary of the far-field zone as a function of the radiation direction, which is determined from the criterion $p(r, \theta) \approx$ const. The directions corresponded to the angles $\theta = 0°$, 10°, 20°, and 30° in the X plane (Fig. 2a). Here, the distance r_d was measured from the previously found calculated radiation center for the direction $\theta = 0°$. The calculation results are shown in Fig. 7. For $\theta = 0°$, the distance to the boundary of the far-field zone corresponds to $r_d \approx 1.26$ m; for $\theta = 10°$, $r_d \approx$ 1.5 m; and for $\theta = 20°$ and $\theta = 30°$, $r_d \approx 2.1$ and $\approx$1.5 m, respectively. When the curves for the directions $\theta =$ 10°, 20°, 30° were calculated, the point $r_0 = (x_0, y_0, z_0) =$ (0, 0, 24 cm) that corresponded to the radiation center for the direction $\theta = 0°$ was taken as the center of a spherical coordinate system.

Using the radiation center that was found in the calculation and experiment, the radiation patterns (RPs) were obtained according to the peak electric-field strength in two perpendicular planes X and Y (Fig. 2a). Measurements of the RPs were performed in the far-field zone in an anechoic chamber. The time dependences of the radiation pulses in the far-field

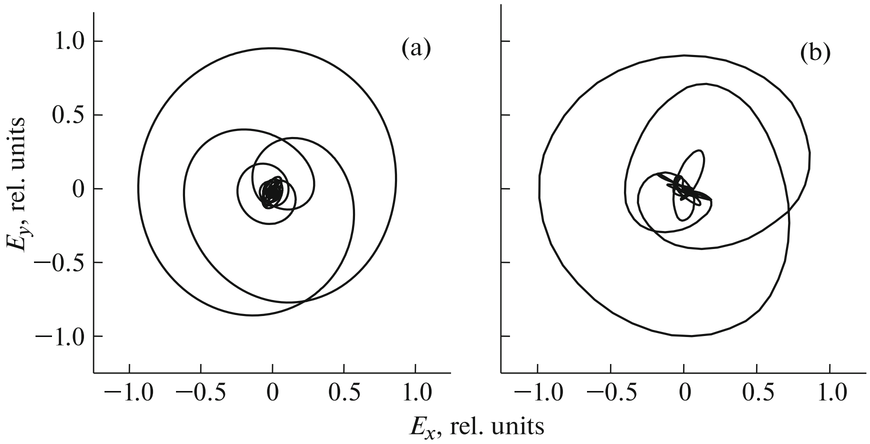

Fig. 6. (a) The calculated and (b) experimental hodographs of the electric-field strength vector along the axis of the conical helical antenna at a distance of 2.8 m from the shield.

zone were calculated using the Kirchhoff representation [13]. Figures 8a and 8b show the normalized calculated (curves *1*) and experimental (curves *2*) RPs corresponding to the peak electric-field strength E_p in the X and Y planes, respectively. The maximum in the calculated and experimental RPs deviates from the direction $\theta = 0°$. This can be explained by the fact that in the conical antenna excited by a UWB pulse, all three radiation modes are simultaneously realized: “normal,” axial, and “multiray” [10]. The turns of the conical antenna with the smaller diameters in comparison with the wavelength in the pulse spectrum radiate in the “normal” mode, while the turns of the antenna with a diameter that exceeds the wavelength in the spectrum radiate in the “multiray” mode, thus leading to an RP asymmetry with respect to the axis $\theta = 0°$.

The angular dependences of the coefficient of ellipticity on the direction θ in the X and Y planes were obtained. Figures 8a and 8b show the calculated (curves *3*) and experimental (curves *4*) angular dependences of the coefficient of ellipticity $p(\theta)$ that were measured in the X and Y planes, respectively. Because the considered conical helical antenna has no axial symmetry, studies of the polarization diagrams $p(\theta)$ in a certain plane at a fixed distance from the radiation center showed their asymmetry with respect to the direction $\theta = 0°$. The polarization diagrams in the X and Y planes are also different.

The shape of a UWB radiation pulse depends on the angle of observation. Using the results of the numerical simulation, the angular dependences of the root-mean-square (rms) deviation σ of the pulse shape in a preset direction θ on the pulse shape in the direction $\theta = 0°$ in the X (Fig. 9a) and Y planes (Fig. 9b) were found for the horizontal (curves *1*) and vertical (curves *2*) polarizations. The distance from the radiation center ($r_0 = 24$ cm) to the observation point was $r = 3$ m. The rms deviation values were calculated from the following formula:

$$\sigma = \sqrt{\frac{\sum_{i=1}^{T}\left(u(t_i) - v(t_i)\right)^2}{\sum_{i=1}^{T} v^2(t_i)}},$$

where $u(t_i) = U(t_i)/\max_T |U(t_i)|$ is the normalized function of the pulse in a given direction, $v(t_i) = V(t_i)/\max_T |V(t_i)|$ is the normalized function of the pulse in the direction $\theta = 0°$, and T is the length of the series in time. The angular dependence of the rms deviation showed that the shapes of pulses in symmetric directions (relative to $\theta = 0°$) do not coincide; this confirms the data that were obtained for the polarization diagrams $p(\theta)$.

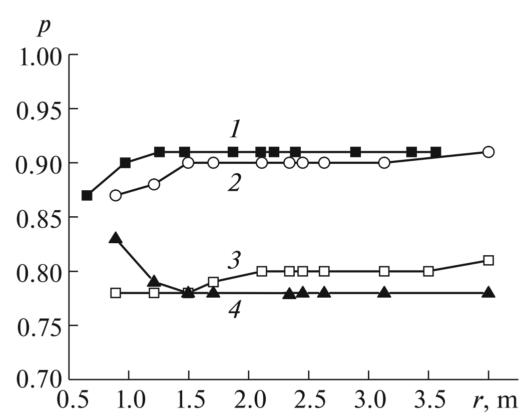

Fig. 7. The calculated dependences of the coefficient of ellipticity on the distance in different directions in the X plane: $\theta = 0°$ (*1*), 10° (*2*), 20° (*3*), and 30° (*4*).

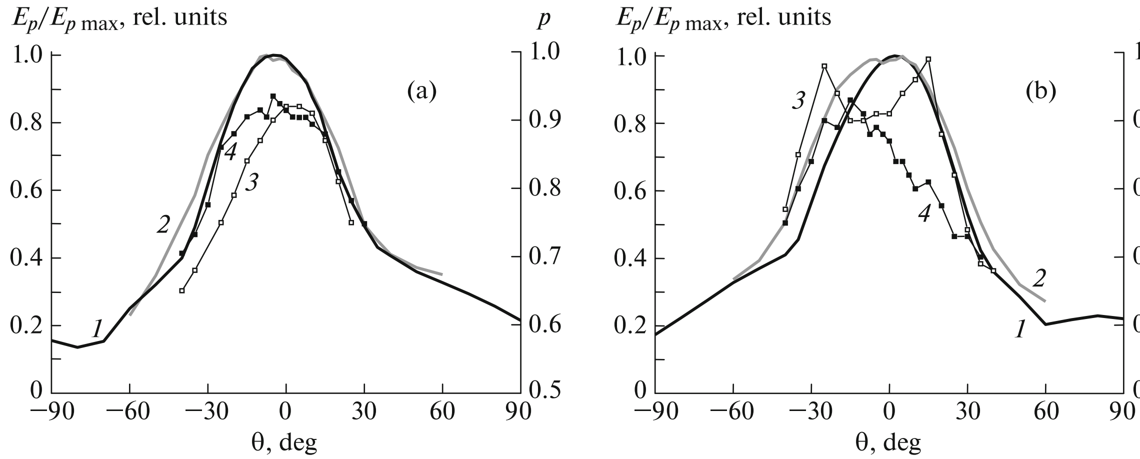

Fig. 8. The (*1*) calculated and (*2*) experimental normalized radiation patterns of the peak field strength and the (*3*) calculated and (*4*) experimental angular dependences of the coefficient of ellipticity in two perpendicular *X* (a) and *Y* (b) planes.

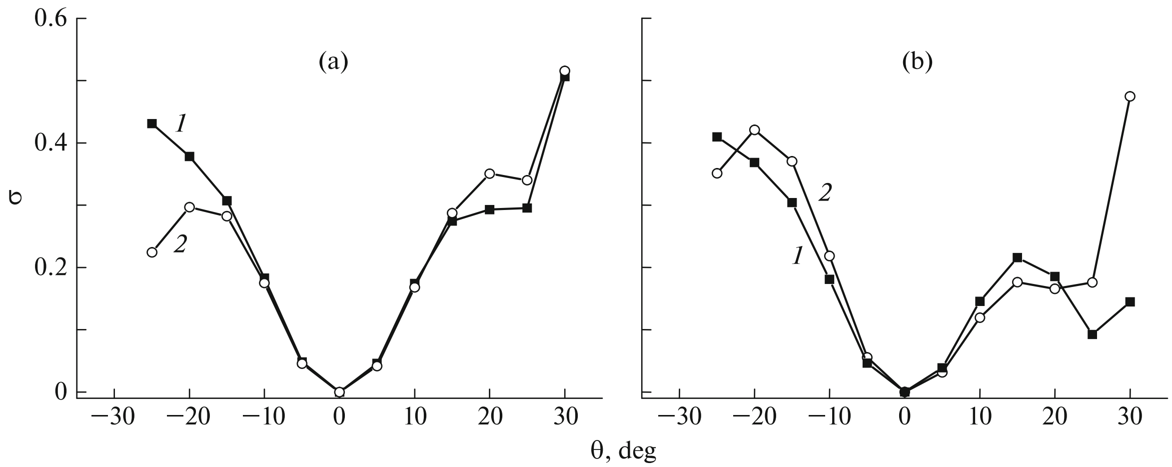

Fig. 9. The angular dependences of rms deviation of pulses in a specified angular direction on the pulse shape in the direction θ = 0° for the (*1*) horizontal and (*2*) vertical polarizations in the *X* (a) and *Y* (b) planes.

3. RADIATION OF HIGH-POWER UWB PULSES

In high-voltage measurements, the amplitudes of a bipolar excitation pulse with a duration of 1 ns were −194/+188 kV. A TEM asymmetric horn was used to receive pulses. The shapes of radiation pulses were recorded in the experiment along the antenna axis (Fig. 10a) for the horizontal (curve *1*) and vertical (curve *2*) components of the electric field. The receiving TEM antenna was located at a distance of 5 m from the radiator. A hodograph of the electric-field strength vector **E** was constructed according to these data (Fig. 10b). The coefficient of ellipticity was $p \cong 0.9$. The peak field strength E_p was found from the hodograph, and the effective radiation potential was calculated; its value was $rE_p \cong 270$ kV. In this case, the antenna efficiency with respect to the peak field strength was $k_E = rE_p/U_{g\max} = 1.35$, where $U_{g\max}$ is the maximum amplitude of a bipolar voltage pulse from the generator. The energy efficiency of the antenna that is determined as the ratio of the radiated energy to the bipolar-pulse energy at the antenna input was evaluated from the experimental data as in [8]; its value was $k_w = 0.85$.

CONCLUSIONS

The optimal geometry of a conical helical antenna for radiating a bipolar pulse with a duration of 1 ns was chosen. Numerical and experimental investigations of the antenna characteristics in the frequency and time domains were performed. The frequency overlap factor at a VSWR level of ≤2 was $b = 3.85$. The position of the antenna radiation center and the boundary of the far-field zone were estimated on the basis of the

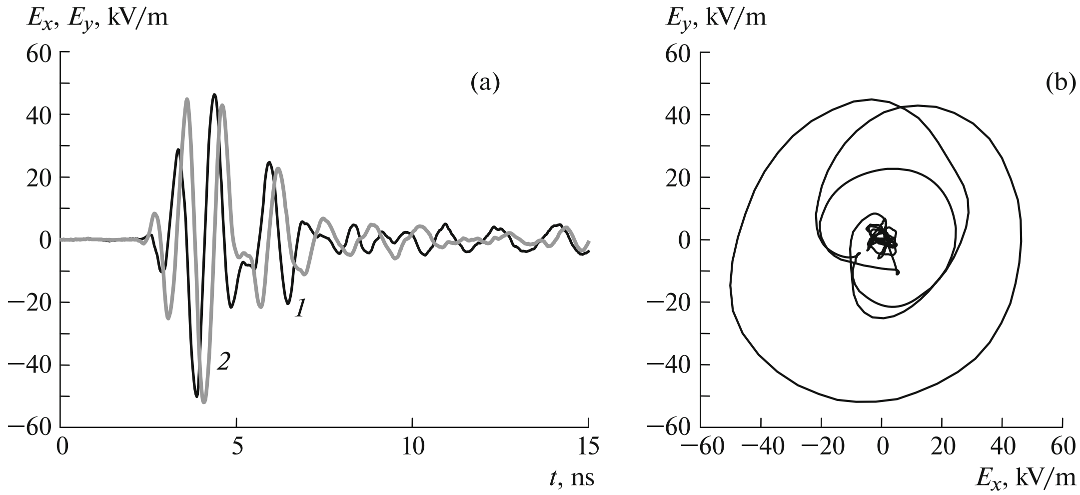

Fig. 10. Oscillograms of radiation pulses for the (*1*) horizontal and (*2*) vertical field components that were obtained (a) in the direction $\theta = 0°$ at a distance of 5 m from the shield and (b) the corresponding hodograph of the electric-field strength vector.

previously proposed criteria. It was shown that the radiated-pulse shape and the coefficient of ellipticity depend on the angle θ and the chosen radiation plane.

A high-power UWB radiation source with elliptical polarization was created using the developed antenna. The source operated at a pulse repetition frequency of 100 Hz. The amplitude of a high-voltage bipolar voltage pulse was approximately 190 kV. The coefficient of ellipticity that was measured in the far-field zone along the antenna axis was $p \cong 0.9$. The effective radiation potential of the source was $rE_p = 270$ kV. The obtained energy and peak field-strength efficiencies were $k_w = 0.85$ and $k_E = 1.35$, respectively. Note that the use of the conical helical antenna made it possible to increase the energy efficiency in comparison with a cylindrical helical antenna ($N = 4$), whose energy efficiency was $k_w = 0.75$ [8].

REFERENCES

1. Gubanov, V.P., Efremov, A.M., Koshelev, V.I., Kovalchuk, B.M., Korovin, S.D., Plisko, V.V., Stepchenko, A.S., and Sukhushin, K.N., *Instrum. Exp. Tech.,* 2005, vol. 48, no. 3, p. 312.
2. Efremov, A.M., Koshelev, V.I., Kovalchuk, B.M., Plisko, V.V., and Sukhushin, K.N., *Instrum. Exp. Tech.,* 2011, vol. 54, no. 1, p. 70. doi 10.1134/S0020441211010052
3. Belichenko, V.P., Buyanov, Yu.I., and Koshelev, V.I., *Sverkhshirokopolosnye impul'snye radiosistemy* (Ultrawideband Pulse Radio Systems), Artech House, Boston and London 2017; Novosibirsk: Nauka, 2015.
4. Efremov, A.M., Koshelev, V.I., Kovalchuk, B.M., Plisko, V.V., and Sukhushin, K.N., *Laser Part. Beams*, 2014, vol. 32, no. 3, p. 413. doi 10.1017/S0263034614000299
5. Mayes, J.R., Mayes, M.G., Nunnaly, W.C., and Hatfield, C.W., *Proc. 17th IEEE Inter. Pulsed Power Conf.,* Washington, 2009, p. 484.
6. Delmote, P., Pinquet, S., and Bieth, F., in *Ultra-Wideband, Short-Pulse Electromagnetics,* Sabath, F. and Mokole, E.L., Eds., (New York, Springer Science + Business Media, 2014), vol. 10, pp. 239–250. doi 10.1007/978-1-4614-9500-0_22
7. Morton, D., Banister, J., DaSilva, T., Levine, J., Naff, T., Smith, I., Sze, H., Warren, T., Giri, D.V., Mora, C., Pavlinko, J., Schleher, J., and Baum, C.E., *Proc. 2010 Inter. Power Modulator and High Voltage Conf.,* Atlanta, GA, 2010, p. 186.
8. Andreev, Yu.A., Efremov, A.M., Koshelev, V.I., Kovalchuk, B.M., Petkun, A.A., Sukhushin, K.N., and Zorkaltseva, M.Yu., *Rev. Sci. Instrum.,* 2014, vol. 85, no. 10, p. 104703. doi 10.1063/1.4897167
9. Andreev, Yu.A., Efremov, A.M., Koshelev, V.I., Kovalchuk, B.M., Plisko, V.V., Sukhushin, K.N., and Zorkaltseva, M.Yu., *Laser Part. Beams,* 2015, vol. 33, no. 4, p. 633. doi 10.1017/S0263034615000725
10. Chatterjee, J.S., *J. Appl. Phys.,* 1953, vol. 24, no. 5, p. 550.
11. Yurtsev, O.A., Runov, A.V., and Kazarin, A.N., *Spiral'nye antenny* (Helical Antennas), Moscow: Sovetskoe Radio, 1974.
12. Balzovskii, E.V., Buyanov, Yu.I., and Koshelev, V.I., *J. Commun. Technol. Electron.,* 2010, vol. 55, no. 2, p. 172.
13. Zorkaltseva, M.Yu., Koshelev, V.I., and Petkun, A.A., *Izv. Vyssh. Uchebn. Zaved. Fiz.,* 2014, vol. 57, no. 12/2, p. 27.

Translated by A. Seferov